Received: 13 October 2023 | Revised: 13 December 2023 | Accepted: 22 December 2023

DOI: 10.1111/gtc.13094

ORIGINAL ARTICLE

Genes to Cells WILEY

GTP-dependent regulation of heterochromatin fluctuations at subtelomeric regions in *Saccharomyces cerevisiae*

Takahito Ayano[1,2] | **Takuma Yokosawa**[1] | **Masaya Oki**[1,3]

[1]Department of Applied Chemistry and Biotechnology, Graduate School of Engineering, University of Fukui, Fukui, Japan

[2]Research Fellowships of Japan Society for the Promotion of Science for Young Scientists (JSPS), Tokyo, Japan

[3]Life Science Innovation Center, University of Fukui, Fukui, Japan

Correspondence
Masaya Oki, Department of Applied Chemistry and Biotechnology, Graduate School of Engineering. University of Fukui, Fukui, Japan.
Email: ma4sa6ya@u-fukui.ac.jp

Funding information
Japan Society for the Promotion of Science London; JSPS KAKENHI, Grant/Award Numbers: JP21J15569, JP22H02301; Institute for Fermentation, Osaka (IFO), Grant/Award Number: G-2022-2-18

Communicated by: Takehiko Kobayashi

Abstract

In eukaryotes, single cells in a population display different transcriptional profiles. One of the factors regulating this heterogeneity is the chromatin state in each cell. However, the mechanisms of epigenetic chromatin regulation of specific chromosomal regions remain unclear. Therefore, we used single-cell tracking system to analyze *IMD2*. *IMD2* is located at the subtelomeric region of budding yeast, and its expression is epigenetically regulated by heterochromatin fluctuations. Treatment with mycophenolic acid, an inhibitor of de novo GTP biosynthesis, triggered a decrease in GTP, which caused heterochromatin fluctuations at the *IMD2* locus. Interestingly, within individually tracked cells, *IMD2* expression state underwent repeated switches even though *IMD2* is positioned within the heterochromatin region. We also found that 30% of the cells in a population always expressed *IMD2*. Furthermore, the addition of nicotinamide, a histone deacetylase inhibitor, or guanine, the GTP biosynthesis factor in salvage pathway of GTP biosynthesis, regulated heterogeneity, resulting in *IMD2* expression being uniformly induced or suppressed in the population. These results suggest that gene expression heterogeneity in the *IMD2* region is regulated by changes in chromatin structure triggered by slight decreases in GTP.

KEYWORDS

GTP, heterochromatin, *IMD2*, *Saccharomyces cerevisiae*, single cell

1 | INTRODUCTION

Gene expression is regulated by chromatin structure. In regions of active genes, nucleosomes are separated from each other, creating a relaxed chromatin structure known as euchromatin. In contrast, within regions where gene are silenced, individual nucleosomes converge, forming a condensed chromatin structure known as heterochromatin. These characteristic chromatin structures are stably maintained and transmitted across cell divisions. However, not all chromatin states are maintained throughout life; chromatin structures can change during development and differentiation due to changes in gene expression patterns.

In *Saccharomyces cerevisiae*, the *HM*, rDNA, and telomere regions are known to be transcriptionally silenced (Gartenberg & Smith, 2016; Rusche et al., 2003; Sun et al., 2011). The rDNA region is silenced by the

Sir2-containing RENT complex (Ghidelli et al., 2001; Smith & Boeke, 1997), whereas in the *HM* and telomere regions, the Sir2/3/4 complex forms and maintains hypoacetylated heterochromatin by means of Sir2-mediated deacetylation of H4K16. It has also been recently reported that the maintenance of stable silencing state at *HM* region is dependent on the amount of Sir4 (Saxton & Rine, 2022). However, if the heterochromatin region continues to expand, it also represses essential genes; therefore, boundaries are formed at chromosomes to inhibit Sir complex-mediated spreading (Kamata et al., 2023; Oki et al., 2004; Oki & Kamakaka, 2002). The reported boundary-formation mechanisms depend on DNA sequence, such as the *CHA1* gene promoter downstream of *HML* (Donze & Kamakaka, 2001) and the threonine transfer RNA (tRNA) gene near *HMR* (Donze et al., 1999; Donze & Kamakaka, 2001). In these characteristic sequences, nucleosome-free regions form and serve as boundaries (Oki & Kamakaka, 2005). Modified histones may also act as boundaries. For example, H4K16 acetylation by Sas2 forms a boundary that prevents heterochromatin elongation at some telomeres (Kimura et al., 2002; Kimura & Horikoshi, 2004; Suka et al., 2002).

Using budding yeast, we have developed a system to track gene expression states in single cells and have shown that heterochromatin spreading is regulated by boundaries (Mano et al., 2013). Still, boundaries fluctuate in response to the environment and cause heterochromatin regions to spread and contract, resulting in the epigenetic regulation of the expression state of nearby genes. However, the physiological significance of fluctuations of heterochromatin regions has yet to be clarified.

Contrary to budding yeast, heterochromatin in fission yeast is formed in an H3K9me-dependent manner, and anti-silencing factors suppress ectopic heterochromatin formation. Epimutants have been recently reported to have acquired drug resistance in response to caffeine by changing the chromatin structure and forming novel heterochromatin regions (Torres-Garcia et al., 2020; Yaseen et al., 2022). It has also been reported that small RNAs epimutants were generated spontaneously in *Caenorhabditis elegans* over the course of generations (Beltran et al., 2020; Wilson et al., 2023). Thus, epimutants are tolerant to environmental changes and necessary for homeostasis, but detailed mechanism by which epimutants occur remain elucidated.

In this study, we focused on *I*nosine *M*onophosphate *D*ehydrogenase 2 (*IMD2*), which encodes an inosinate dehydrogenase (IMPDH) that catalyzes the reaction from inosinic (IMP) to xanthosinic acid (XMP) through a de novo GTP biosynthetic pathway (Hedstrom, 1999; Woods et al., 1983). Budding yeast has the additional *IMD2* paralogs *IMD1*, *IMD3*, and *IMD4* (Hyle et al., 2003). Among these *IMD* gene families, the IMPDH encoded by *IMD2* (Imd2) only has a unique amino acid structure that makes it resistance to mycophenolic acid (MPA), a GTP biosynthesis inhibitor. Therefore, *IMD2* is essential for growth in high concentration of MPA (Jenks & Reines, 2005; McPhillips et al., 2004; Shaw et al., 2001). *IMD2* is also under the control of a unique DNA sequence-dependent transcriptional regulatory mechanism in response to GTP depletion. Initially, when GTP is abundant in the cell, transcription is attenuated in the repressor element (RE) region, and *IMD2* is not expressed (Davis & Ares Jr., 2006; Kopcewicz et al., 2007; Steinmetz et al., 2006). However, when MPA or other factors reduce GTP levels, the transcription start site switches from upstream to downstream of the RE (Connell et al., 2022; Escobar-Henriques et al., 2003; Escobar-Henriques & Daignan-Fornier, 2001; Jenks et al., 2008; Kuehner & Brow, 2008; Shaw & Reines, 2000). Thereby, *IMD2* expression is regulated to maintain constant GTP levels in vivo. *IMD2* is also located near telomeres on the right arm of chromosome VIII and is influenced by the repressive activity of the Sir complex (Ellahi et al., 2015; Mitsumori et al., 2016). Thus, *IMD2* bears DNA sequences that depend on transcriptional regulation and are also predicted to undergo epigenetic regulation of gene expression through heterochromatin formation.

In this study, we focused on *IMD2* and analyzed its heterochromatin fluctuations at the subtelomeric region by single-cell tracking using a fluorescent protein as a reporter to identify novel heterochromatin regulatory mechanisms that respond to GTP levels.

2 | RESULTS

2.1 | IMD2 silencing is reversed in a GTP-dependent manner

To identify genes affected by fluctuations in heterochromatin regions, we performed microarray-based gene expression analysis using strains with disrupted *SIR2*, *SIR3*, and *SIR4*, well-known markers of heterochromatin. Additionally, we carried out chromatin immunoprecipitation (ChIP) on chip analysis, focusing on the specific localized region of Sir3 (Mitsumori et al., 2016). From these results, we selected *IMD2*, which is located at the telomere-proximal region of the right arm of chromosome VIII (Figure 1a). *IMD2* encodes IMPDH, which is involved in de novo GTP biosynthesis, and its expression can be induced by MPA, an inhibitor of GTP biosynthesis. Next, to confirm whether the Sir complex represses *IMD2* expression, we measured the expression level of *IMD2* by RT-qPCR using wild-type (WT) and *SIR2*

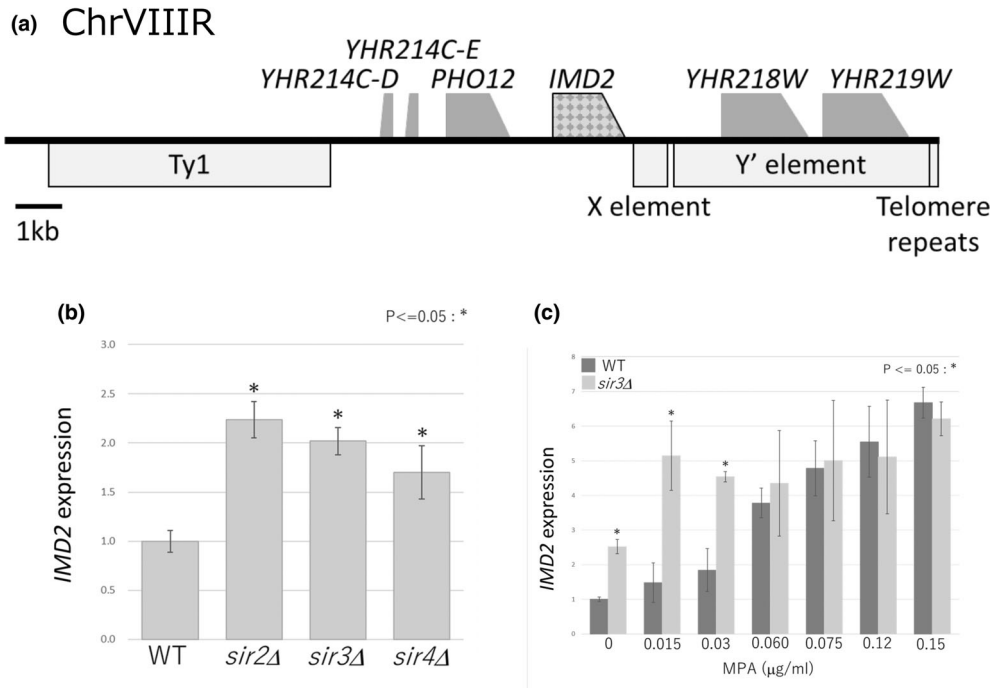

FIGURE 1 *IMD2* silencing is released in a GTP-dependent. (a) Schematic diagram showing the last 20 kb of the right arm of chromosome VIII. (b) *IMD2* expression was analyzed by RT-qPCR. Data were normalized to the wild-type (WT). Asterisks indicate $p < .05$ compared with the WT (Student's *T*-test). (c) *IMD2* expression levels upon treatment with mycophenolic acid (MPA) were analyzed by RT-qPCR. Data were normalized to WT (MPA 0 μg/mL). Asterisks indicate $p < .05$ compared with the WT at each MPA concentration (Student's *T*-test).

(*sir2Δ*), *SIR3* (*sir3Δ*), and *SIR4* (*sir4Δ*) deletion strains (Figure 1b). We found that *IMD2* expression was upregulated in each *SIR* disruption strain compared with the WT, indicating that *IMD2* expression is regulated by the Sir complex.

Since *IMD2* expression is induced in response to a decrease in GTP, we hypothesized that heterochromatin fluctuations at the *IMD2* region would also depend on GTP amount and analyzed changes in expression levels as a function of MPA concentration in WT and *sir3Δ* strains (Figure 1c). At 0.060 μg/mL MPA, the *IMD2* expression level in the WT increased to the same level as that in *sir3Δ*, indicating that *IMD2* silencing is reversed at 0.060 μg/mL MPA. These results suggested the presence of a regulatory mechanism that senses GTP depletion or reduction, and acts on heterochromatin at the *IMD2* region at an earlier stage than that of the DNA sequence-dependent transcriptional regulation reported by Brow et al. (Kuehner & Brow, 2008).

2.2 | Heterochromatin stability differs from cell to cell

To track changes in *IMD2* expression in individual cells, we developed a yeast strain to be used with our previously-developed single-cell tracking system (Mano et al., 2013). First, we generated strain FUY1584 to serve as an internal control for the quantification of fluorescence intensity, for which a fusion of H2B and the mCherry coding sequence was inserted into the euchromatin region of WT (BY4742) (Figure S1, left panel). Next, we constructed the *IMD2* expression strain (FUY1735) for single-cell tracking experiments. In FUY1735, the *IMD2* promoter region, which regulates DNA sequence-dependent transcription, was retained, and the *IMD2* open reading frame was replaced by *H2B-EYFP* (Figure S1, right panel). To test whether deletion of *IMD2* affects growth, we added MPA to FUY1735 and confirmed that no abnormal growth effect was observed (Figure S2). This suggests that while the addition of low concentrations of MPA induces *IMD2* expression, it does not impact cell growth. Thus, we tested the extent at which different concentrations of MPA (0, 0.015, 0.075, and 0.150 μg/mL) induced expression in individual cells. To do this, tracking was initiated with a single cell, and MPA was added after 5 h and followed until 15 h (Figure 2a, Movie EV1, EV2, EV3, and EV4). We observed that EYFP increased as a function of MPA concentration, indicating that *IMD2* expression, induced by MPA, can be quantified at the single-cell level. Therefore, we randomly selected 10 cells for each MPA concentration and quantified the expression state changes from 0 to 12 h at hourly intervals (Figure 2b). We found that induction of *IMD2* expression depended on MPA concentration, but its expression level after induction differed from cell to cell. This result suggests that the stability of heterochromatin in the *IMD2* region varies among cells. Interestingly, some of the cells expressed *IMD2* weakly even before the addition of MPA. This indicates that heterochromatin fluctuations differ from cell to cell before GTP depletion and that GTP regulates the expression level of *IMD2*.

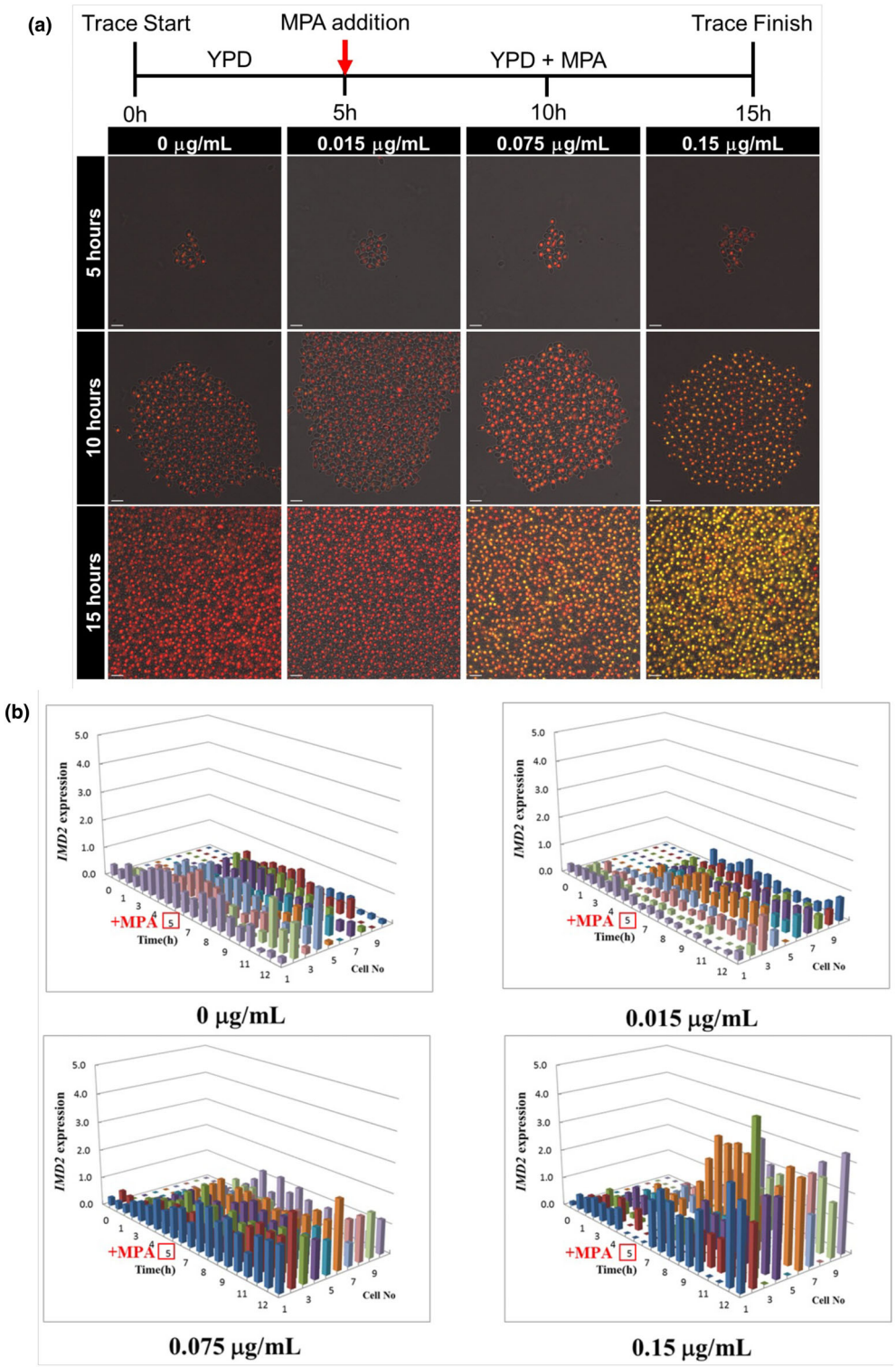

FIGURE 2 GTP-dependent induction of *IMD2* expression differs between individual cells. *IMD2* expression was followed at the single-cell level after the addition of MPA. (a) Single-cell tracking of the FUY1735 strain with mycophenolic acid (MPA) and fluorescent images acquired at each time point (5, 10, and 15 h). Red, mCherry (control); yellow, EYFP (*IMD2*). Scale bars: 10 μm. (b) Ten cells were selected randomly from the tracking results in (a) and the expression status of *IMD2* (EYFP) in each cell was measured.

2.3 | IMD2 is heterogeneously expressed in cell populations

To confirm the expression status of *IMD2* in the absence of MPA or GTP depletion, single-cell tracking was performed in YPD for 10 h at 15 min intervals. We found that the EYFP intensity fluctuated, and the expression state of *IMD2* switched many times despite the absence of the MPA (Figure 3a and Movie EV5). Therefore, we focused on the mother cell that initially expressed *IMD2* and followed its expression status changes across generations. We found that *IMD2* expression decreased gradually in the first 3 h, remained turned off from 3 to 6 h, and increased thereafter (Figure 3b and Movie EV6). To

determine whether the regularity of this expression state was observed in all daughter cells, we quantified the expression change for the mother cell, whose initial expression state was ON, as well as the 29 daughter cells derived from it (Figure 3c, left panel). We found that the *IMD2* expression state varied from cell to cell after

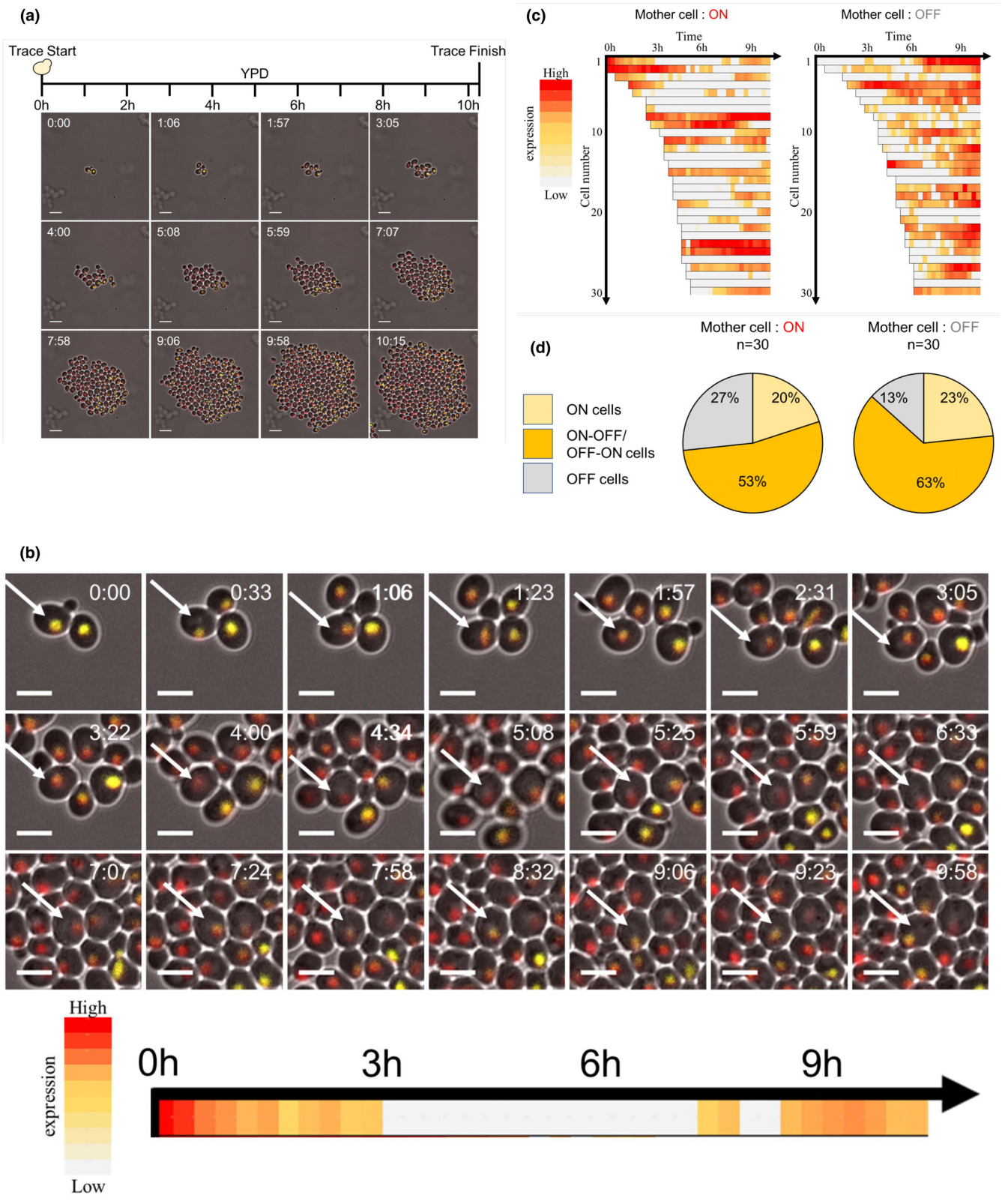

FIGURE 3 Legend on next page.

division, with 20% of cells always expressing *IMD2*, 27% of cells maintaining *IMD2* OFF, and 53% of cells switching between ON and OFF (Figure 3d, left panel). Next, to confirm the influence of the mother cell, we followed mother cells that did not express *IMD2* at the initial stage to examine changes in the expression status of daughter cells (Figure 3c,d, right panel). We observed that the expression status of one mother cell and the 29 daughter cells derived from it included cells that remained ON (23%), cells that remained OFF (13%), and cells that switched between ON and OFF (63%), indicating that the expression status of the mother cell did not affect the daughter cell expression status.

Next, to determine whether the change in *IMD2* expression depends on the cell cycle or happens stochastically, we investigated the initiation of EYFP expression to identify the cell cycle phase. During the cell cycle of budding yeast, small protrusions emerge from G1 to S phase, followed by the growth of daughter cells in size throughout S phase, and culminating in mitosis during G2/M phase. This progression in cell morphology allows for the determination of the cell cycle. Among the 30 cells whose initial mother cell was ON, the cell cycle was delineated based on the morphology before and after the transition in 13 cells where the expression changed from OFF to ON (Figure 4a). EYFP expression was induced from G1 to early S phase of the cell cycle. We then focused on the ratio of ON/OFF cells in the cell population with fluctuating expression status, which changes with proliferation. The percentage of ON cells in the population was measured at 15 min intervals for 2.5 h after the overall cell number reached ≥30 cells (Figure 4b). Interestingly, the percentage of ON cells in the cell population remained almost constant (30%–40%), even while the cells proliferated. To explore the regulatory mechanisms governing ON cells within these populations, we overexpressed *SIR3* (*SIR3* OE) and assessed its impact on both the proportion of ON cells and the heterogeneous expression status of *IMD2* among the cell population. During single-cell tracking analysis with the *SIR3* OE strain in YM-uracil +2% galactose media, we analyzed the percentage of ON cells every 30 min once the cell count surpassed 30 cells. Our findings revealed that the overexpression of *SIR3* led to an increased repression of *IMD2* and a decrease in the rate of ON cells (<10%) within the cell population (Figure S3). These results indicate that *IMD2* expression is influenced not only by the cell cycle in individual cells but also by the chromatin state of each cell.

2.4 | IMD2 expression is regulated by histone deacetylases and GTP

To unravel the expression regulatory mechanism upon GTP depletion at the *IMD2* region, we studied the effect of the Sir complex, which is required for heterochromatin formation. We generated a *sir3Δ* strain (FUY1807) and performed single-cell tracking in YPD (Figure 5a and Movie EV7). We started a culture from one cell and tracked all cells for 10 h at 15 min intervals to measure the expression level of EYFP in each cell (Figure 5b). We found that EYFP was highly expressed in all cells. On the flip side, *IMD2* was inhibited in nearly all cells within the *SIR3* OE strain (Figures S4 and S5). These results indicate that the Sir complex reversibly regulates *IMD2* expression. Therefore, we investigated whether the histone deacetylase (HDAC) activity of Sir2, a component of the Sir complex, is essential in regulating the expression state diversity at the *IMD2* region. Nicotinamide (NAM), an HDAC inhibitor of Sir2, was added to the WT strain to confirm its effect at the single-cell level (Figure 5c and Movie EV8) (Avalos et al., 2005; Bitterman et al., 2002; Imai et al., 2000). Single-cell tracking was performed at 15 min intervals, and the EYFP fluorescence intensity was measured in each cell. We observed that the EYFP expression level was different in each cell for the first 8 h in YPD, indicating diverse expression states among cells (Figure 5d). However, 1 h after NAM transduction, EYFP expression was induced in all cells, akin to the outcomes observed in the *sir3Δ*, with no noted cell-to-cell heterogeneity. These results suggest that the HDAC activity of Sir2 regulates the heterogeneous expression states at the *IMD2* region in individual cells. Next, we confirmed

FIGURE 3 *IMD2* is expressed heterogeneously in cell populations. Single-cell tracking of the FUY1735 fluorescent strain without MPA. (a) Image tracking of a single cell in a population. Scale bars: 10 μm. (b) Upper panel: image tracking of a single cell. Lower panel: expression state of a single cell. Horizontal axis indicates time. The expression state intensity is shown as follows: gray (OFF), yellow (ON, low), and red (ON). The white arrow indicates the single cell being tracked. Scale bars: 5 μm. (c) Expression state of individual cells in the cell population. Left panel: expression status tracking of a population derived from a single ON cell. Right panel: expression status tracking of a population derived from a single OFF cell. The horizontal axis indicates the time, and the vertical axis indicates the number of cells. The intensity of the expression state is shown as follows: gray (OFF), yellow (ON, low), and red (ON). (d) Cell expression state classified into three types: ON, OFF, and ON-to-OFF/OFF-to-ON. The percentage of cells in the cell population is shown in (c). Left panel: cell population tracked from an initial ON cell. Right panel: cell population tracked from an initial OFF cell.

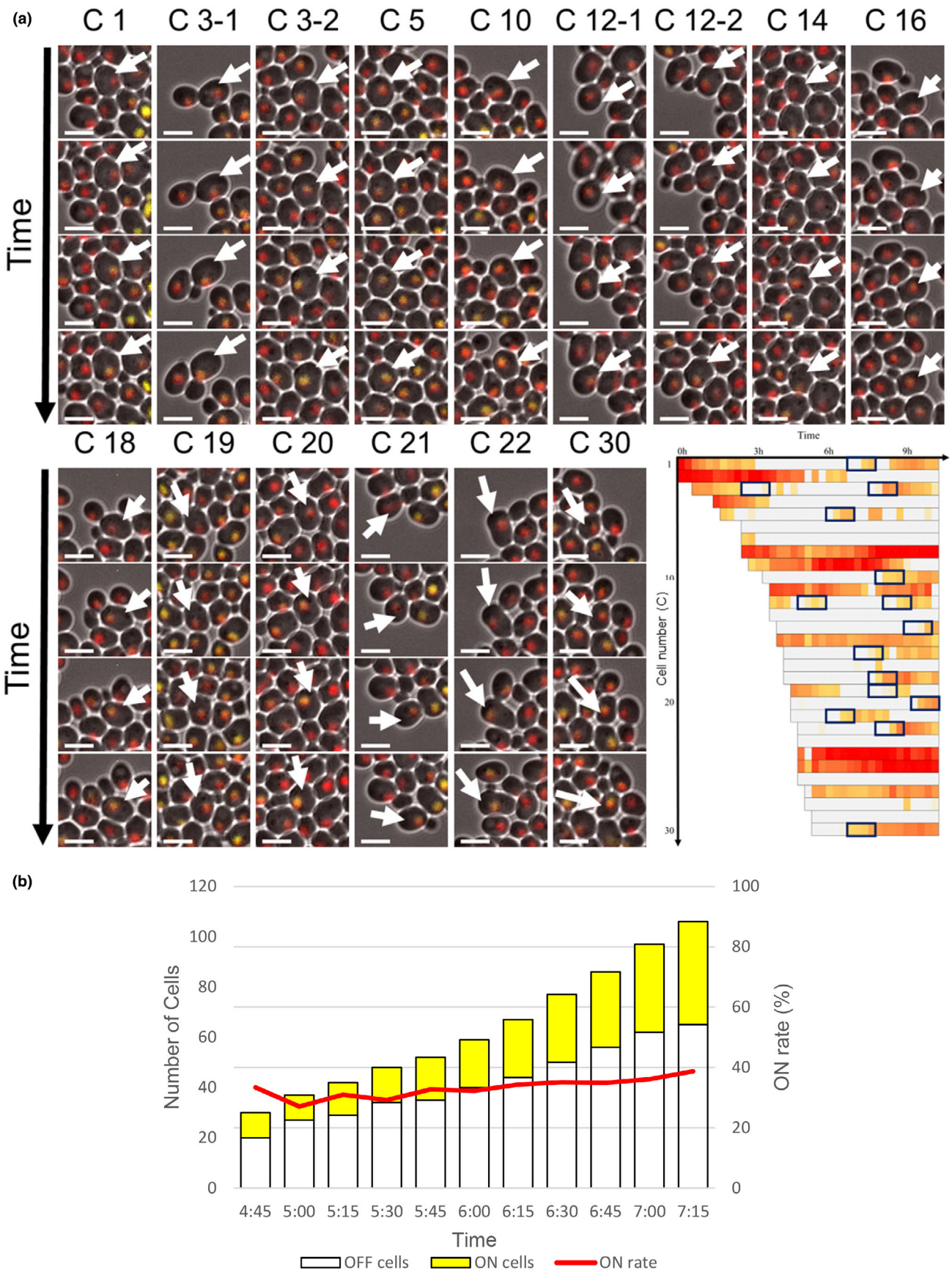

FIGURE 4 Legend on next page.

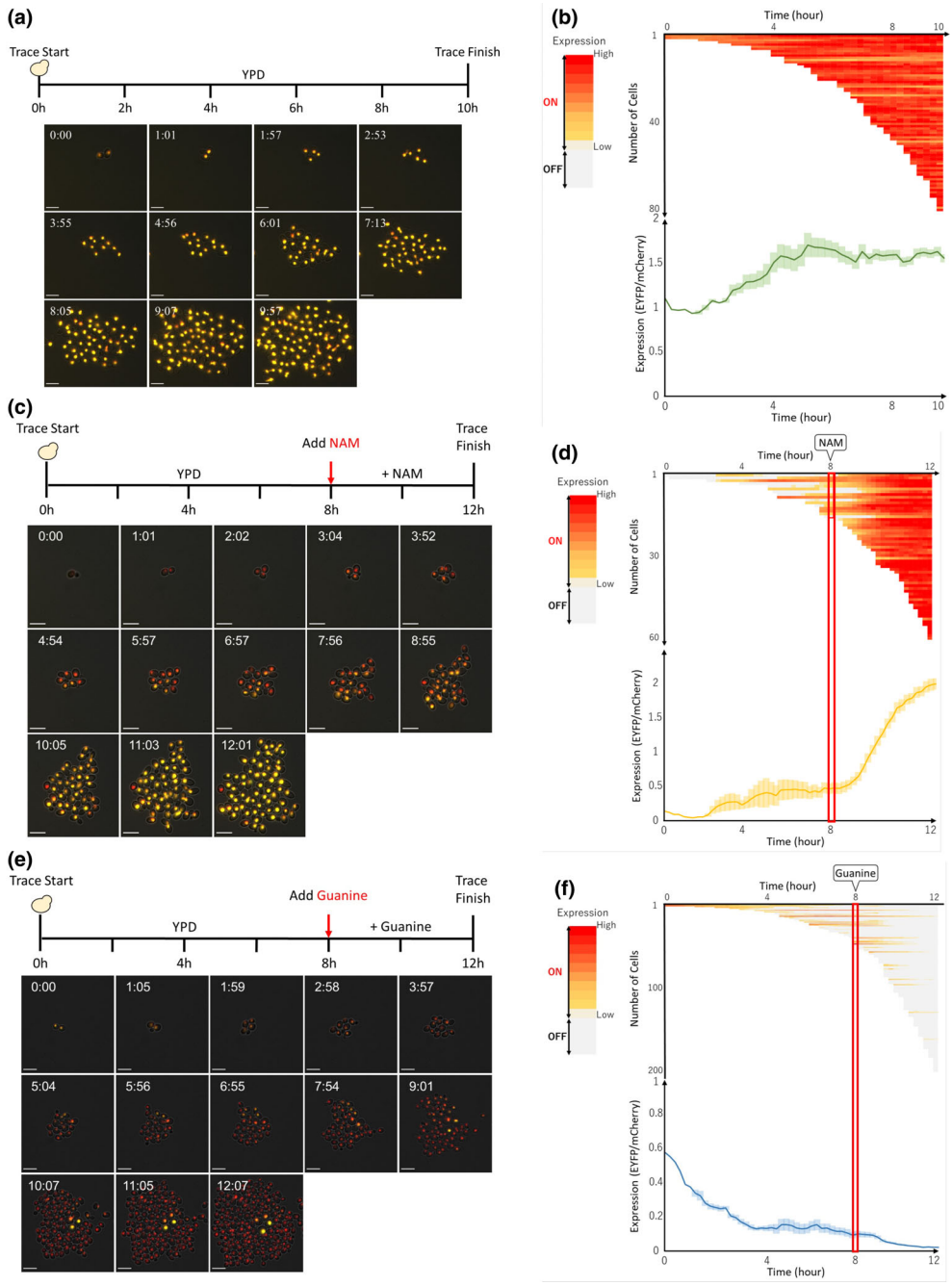

FIGURE 5 Histone deacetylase (HDAC) and GTP regulate *IMD2* expression. (a) Single-cell tracking image of the *sir3Δ* strain. Scale bars: 10 μm. (b) Expression state analysis of (a). (c) Single-cell tracking image of the wild-type (WT) upon nicotinamide (NAM) treatment. Scale bars: 10 μm. (d) Expression state analysis of (c). The red border indicates the start of the NAM addition. (e) Single-cell tracking results of WT with guanine. Scale bars: 10 μm. (f) Expression state analysis of (e). The red rectangle indicates the start of guanine addition. In (b), (d), and (f), Upper panel: expression state change in one cell (gray [OFF]; yellow [ON, low]; and red [ON]). The horizontal axis represents the time, and the vertical axis represents the cell number. Lower panel: the expression level change of a cell population is indicated by a line graph. The horizontal axis represents the time, and the vertical axis represents the cell number. The average expression level of all cells is shown as a broken line, and the error bars represent the standard deviation.

the GTP effect, which is known to regulate the *IMD2* expression state, by adding guanine, which is required for the salvage pathway of GTP biosynthesis, without IMPDH and performed single-cell tracking. Cultures were started with one cell, guanine at a final concentration of 0.5 mM was added after 8 h of culture, and all

FIGURE 4 *IMD2* expression is regulated in a cell cycle-dependent manner. (a) Images of cells (Figure 3c, left panel) whose expression state was switched from OFF to ON during the tracking, before and after the switch. The images were extracted from the black, framed areas in the lower right panel. Arrows indicate cells that switched expression. The vertical axis represents the time. Scale bars: 5 μm. (b) Percentage of ON cells in the cell population in left panel of Figure 3c. The left vertical axis represents the cell number. ON cells are shown as yellow and OFF cells as white overlaid bars. The right vertical axis indicates the percentage of ON cells relative to the total number of cells. The red line denotes the change in the ON cell rate. The horizontal axis represents the time elapsed after the total number of cells exceeded 30.

cells were followed up until 12 h at 15 min intervals (Figure 5e and Movie EV9). The fluorescence intensity of EYFP in each cell was measured. While there was diversity in the expression state among cells before guanine addition, after guanine addition, EYFP fluorescence was reduced in all cells (Figure 5f). However, individual cells switched EYFP OFF at different times, suggesting that GTP concentrations, and thus *IMD2* expression regulation, differed among cells. These results indicate that heterochromatin in the *IMD2* region of individual cells fluctuates and controls the diverse *IMD2* expression states in response to GTP concentration.

3 | DISCUSSION

Heterochromatin spreads from specific genomic regions, albeit not everywhere. It stops spreading at boundaries, with heterochromatin regions being formed only in specific locations, in which the expression of genes becomes suppressed (Donze et al., 1999; Oki & Kamakaka, 2005). Heterochromatin region undergo fluctuations during cell divisions (Mano et al., 2013), yet the precise mechanism driving these fluctuations in response to both internal and external environmental changes remains unknown. In this study, we found that *IMD2* expression in heterochromatin near telomeres is triggered by GTP decrease in vivo and induced by heterochromatin fluctuations. Considering the widespread presence of bioenergetic synthesis systems such as GTP among eukaryotes, it is plausible that analogous systems governing epigenetic control of energy levels may also exist in other eukaryotic organisms. A more detailed analysis will unveil how gene expression is governed by fluctuations in heterochromatin in vivo and identify the factors that play a role in regulating specific gene expression. This exploration may also lead to the discovery of new mechanisms for regulating gene expression.

Transcription of the *IMD2* gene is regulated by a change in its transcription start site, which depends on GTP level (Kuehner & Brow, 2008). The *IMD2* region has been studied in detail regarding DNA sequence-specific transcriptional regulation, and it is well suited for elucidating regulatory mechanisms of epigenetic gene expression. Here, we showed that the *IMD*2 heterochromatin region responds to GTP levels in vivo (Figures 1c and 2) and suggested that the different expression states of each cell are regulated by cellular GTP abundance, with fluctuating expression states reflecting GTP levels (Figure 5e,f). In fact, *IMD2* expression induction was observed from G1 to early S phase in single cells (Figure 4a). This result suggests that mitotic GTP consumption may have reduced GTP levels in vivo below a threshold level and induced *IMD2* expression. This suggests a mechanism by which the expression state is finely regulated according to the amount of cellular GTP. In addition, the transcription level in the absence of MPA (0 μg/mL) was only about a quarter of that when GTP was depleted or reduced by the addition of MPA (0.060 μg/mL) (Figure 1c). This indicates that expression induction in standard culture cannot compensate for rapid GTP reduction but instead acts to maintain survival. By contrast, expression induction by MPA addition (0.060–0.150 μg/mL) resulted in high expression levels in response to the rapid decrease in GTP. Furthermore, when GTP was depleted to the extent that it interfered with the maintenance of vital functions, *IMD2* may have promoted GTP production to restore cellular homeostasis by sequence-dependent regulation and transcription start site switching (Figure 1c). Thus, *IMD2* is regulated by a three-step mechanism, consisting of a first-step epigenetic regulation of physiologically fluctuating GTP, a second-step epigenetic regulation upon GTP depletion by external stimuli like MPA, and a third-step genetic regulation upon lethal GTP depletion. This three-step expression control mechanism may also regulate GTP abundance in vivo. However, it's crucial to further consider that the observed regulation of heterochromatin by GTP, as previously described, might be indirect. In Figure 2, the variation in *IMD2* expression timing among cells after the introduction of MPA may not directly correlate with the heterochromatin status in each cell. This variation could potentially arise from minor differences in GTP-sensitive pathways, functions related to *IMD2* transcription start sites, cell cycle stages, and other individual cellular factors. In Figure 1c, although our focus centers on a three-step regulation of *IMD2*, it's entirely plausible that the regulation of heterochromatin and the alteration in transcription start sites interact with each other. In the absence of *SIR3* (*sir3Δ*), there was a more significant upregulation observed at MPA 0.03 μg/mL compared with MPA 0 μg/mL, a variation not typically seen in the wild type (WT). This outcome suggests that the Sir protein could potentially hinder the switch in transcription start site from upstream of RE to downstream. In this study, we focused on GTP as a trigger for heterochromatin fluctuation. GTP is not only involved in critical biological phenomena such as nuclear-cytoplasmic transport, DNA synthesis, and cell division, but its levels are also critical for homeostatic survival since excessive GTP causes cells to divide overly. Therefore, it is unsurprising that GTP levels fine-tune the expression of genes

involved in GTP synthesis, such as *IMD2*. Epigenetic regulation of gene expression by heterochromatin fluctuations in response to GTP levels may be conserved between the budding yeast and other eukaryotes, and future analyses are expected to elucidate this possibility.

Although *IMD2* is located within a heterochromatin region, it is always expressed in approximately 30%–40% of cells in a population, regardless of increasing cell numbers due to cell division (Figure 4b). A similar system exists in multicellular organisms like mouse ES cells (Amano et al., 2013; Ko, 2016; Zalzman et al., 2010), in which a given fraction of cells in a dividing population expresses specific genes at certain levels. Remarkably, in unicellular yeast, although the expression state changes in individual cells through cell divisions, the ON expression state is constantly maintained in a stable fraction in the population. Since disruption of *SIR3* turns *IMD2* expression ON in almost all cells, we suggest that *IMD2* expression is regulated by heterochromatin fluctuations. Still, the mechanisms that yeast cells deploy to control the ratio of gene expression states in an entire cell population are currently unclear.

In this study, we also identified cells that expressed *IMD2* even before MPA induction, and found that this normal expression state is epigenetically regulated in a GTP-dependent manner (Figure 3a). However, we did not find out how this expression state affects induction by MPA. For certain genes, once expression is induced, it is induced more strongly and faster than the first time upon re-induction (Bheda et al., 2020). This phenomenon, termed transcriptional memory, has been reported for certain genes, and has been attracting attention in recent years. Thus, it is possible that changes in the expression state of each cell before MPA treatment could have affected subsequent inductions of expression.

We've confirmed the formation and fluctuation of heterochromatin regions in response to GTP, influencing the gene expression state at the *IMD2* region. However, our study didn't identify GTP sensors within the cell, specific cellular regions responsible for GTP sensing, the alterations in chromatin structure at the *IMD2* locus due to reduced GTP levels, or the involved factors. These critical aspects should be addressed in future studies.

4 | EXPERIMENTAL PROCEDURES

4.1 | Yeast strains and plasmids

All yeast strains in this study were based on BY4742 (*MATα his3Δ1 leu2Δ0 lys2Δ0 ura3Δ0*). The *sir3Δ* strain was constructed by homologous recombination using the *KanMX* gene and isolated in a G418 (200 μg/mL) medium (Longtine et al., 1998; Rothstein, 1991). The fluorescent strain for single-cell analysis was constructed by digesting pFOM812 (*HTB1-2* × *mCherry-HIS3*) with *Afe*I and integrating it into the *his3Δ1* locus of BY4742, followed by selection and isolation in YMD (−histidine) medium to generate FUY1584 (Figure 3a, left panel). After digesting pFOM872 (*IMD2*pro-*HTB1-EYFP-IMD2*-ter, *URA3*) with *Hpa*I and integrating it into the *IMD2* locus of FUY1584, the strain was selected in YMD (−uracil) medium, isolated, and designated as FUY1732. FUY1732 was cultured in 5-fluoroorotic acid (5-FOA) medium (Boeke et al., 1984), and the isolated strain was designated as FUY1735 (Figure 3a, right panel). The construction of the *SIR3* overexpression plasmid, pFOM1197, involved cutting pYES2 with *Xba*I and *Bam*HI and then inserting the *SIR3* ORF region. *SIR3* OE strain was produced by transforming FUY1735 with pFOM1197, and this strain was selected in YMD (−uracil) medium. Similarly, a control strain (FUY1735 + Vector) for *SIR3* overexpression experiments was produced transforming FUY1735 with pYES2, also this strain was selected in YMD (−uracil) medium.

G418 added to YPD was used for *KanMX* selection, histidine-free YMD medium for *HIS3* selection, uracil-free YMD medium for *URA3* selection, and 5-FOA medium for *URA3* counterselection, uracil-free YM with 2% galactose for *SIR3* overexpression experiment.

The strains used in this study are listed in Table 1.

TABLE 1 Yeast strains list.

Strain No.	Genotype	Source
FUY737	*MATα his3Δ1 leu2Δ0 lys2Δ0 ura3Δ0 sir4Δ::KanMX*	This study
FUY745	*MATα his3Δ1 leu2Δ0 lys2Δ0 ura3Δ0 sir3Δ::KanMX*	This study
FUY748	*MATα his3Δ1 leu2Δ0 lys2Δ0 ura3Δ0 sir2Δ::kanMX*	This study
FUY838	*MATα his3Δ1 leu2Δ0 lys2Δ0 ura3Δ0*	This study
FUY1584	*MATα leu2Δ0 lys2Δ0 ura3Δ0 his3Δ::HTB1-2xmCherry-HIS3*	This study
FUY1732	*MATα leu2Δ0 lys2Δ0 ura3Δ0 his3Δ::HTB1-2xmCherry-HIS3 imd2Δ::IMD2-URA3-HTB1-EYFP*	This study
FUY1735	*MATα leu2Δ0 lys2Δ0 ura3Δ0 his3Δ::HTB1-2xmCherry-HIS3 imd2Δ::HTB1-EYFP*	This study
FUY1807	*MATα leu2Δ0 lys2Δ0 ura3Δ0 his3Δ::HTB1-2xmCherry-HIS3 imd2Δ::HTB1-EYFP sir3Δ::KanMX*	This study

4.2 | Microarray analysis

Microarray analysis was performed as described previously (Kamata et al., 2023). Yeast strains were grown in YPD medium and collected at the mid-log phase. Total RNA was extracted using the hot phenol method. cRNA was synthesized from 200 ng of total RNA using the GeneChip® 3′ IVT Express Kit (Affymetrix, Santa Clara, CA, USA), and 7.5 μg of cRNA was hybridized for 16 h at 45°C to a GeneChip Yeast Genome 2.0 Array (Affymetrix). GeneChips were washed and stained in Affymetrix Fluidics Station 450, and scanned using GeneChip Scanner 3000 7G System to acquire the data. Data were background-corrected, quantile-normalized, probe set-summarized, and $\log_2$-transformed using Robust Multichip Average default settings (Bolstad et al., 2003; Irizarry, Bolstad, et al., 2003; Irizarry, Hobbs, et al., 2003). Furthermore, based on the annotation information of budding yeast, the signal values of duplicated genes were averaged and summarized, and irrelevant data such as fission yeast-expressed genes were removed.

Microarray data are available in the Gene Expression Omnibus (GEO) under the accession number GSE230739.

4.3 | RNA extraction and RT-qPCR analysis

RNA analysis was performed as described previously (Kamata et al., 2016). Yeast strains were grown in YPD medium at 30°C and collected at the log phase at OD (600 nm) 0.7. When MPA was used, it was added at OD (600 nm) 0.4 and collected at OD (600 nm) 0.7 after 1 h of culture. Total RNA was extracted by the hot phenol method and treated with deoxyribonuclease (RT grade) for Heat Stop (NipponGene, Toyama, Japan). cDNA was prepared using the High Capacity cDNA Reverse Transcription Kit (Applied Biosystems, Foster City, CA, USA). RT-qPCR was performed using the Applied Biosystems StepOnePlus Real Time PCR System (Applied Biosystems) and Power SYBR Green PCR Master Mix (Thermo Fisher Scientific, Carlsbad, CA, USA). The expression level of *IMD2* was normalized based on that of *ACT1*. For each RT-qPCR dataset, three or more replicate experiments were performed, and the average expression levels and standard errors were calculated.

PCR steps were as follows: 10 min at 95°C (one cycle); 15 s at 95°C; and 1 min at 60°C (40 cycles).

The primers used for real-time PCR are listed in Table 2.

TABLE 2 Primers for RT-qPCR list.

Primer name	Sequence
ACT1-F	TCGTTCCAATTTACGCTGGTT
ACT1-Rv	CGGCCAAATCGATTCTCAA
IMD2-F	TGTCGTTGACAAAGGATCCATTA
IMD2-Rv	GCCGATGTCTTGACAGGAATGT

4.4 | Single-cell tracking analysis

Experiments were performed as previously described (Kanada et al., 2020; Mano et al., 2013). Yeast strains were grown in YPD medium at 30°C, and cells were collected at log growth phase of OD (600 nm) 0.2–0.8. For live cell imaging, the collected cells were trapped on CellASIC ONIX plates for haploid yeast cells (four chambers, 3.5–5 μm) (Y04C-02-5PK) (Merck KGaA, Darmstadt, Germany) using the CellASIC ONIX2 Microfluidic System (CAX2-S0000) (Merck) and medium flow at a rate of 2.0 psi. In *SIR3* overexpression experiments, uracil-free YM with 2% galactose media was used instead of YPD.

Single-cell imaging was performed using an Axio Observer Z1 (Carl Zeiss, Oberkochen, Germany) microscope with a 40× Plan-Neofluar objective lens of 1.3 numerical aperture, and image analysis was performed using Axio Vision 4.7.1 (Carl Zeiss) or ZEN 2.3 (blue edition) (Carl Zeiss). *IMD2* (*EYFP*) expression was calculated using the maximum fluorescence intensity in cell and cell-free regions (BG: background) at each imaging point, using the following formula:

$$IMD2\,\text{expression} = \frac{\text{EYFP}_{\text{max}}^{\text{in cell}} - \text{EYFP}_{\text{max}}^{\text{BG}}}{\text{mCherry}_{\text{max}}^{\text{in cell}} - \text{mCherry}_{\text{max}}^{\text{BG}}}.$$

MPA (0.015, 0.075, 0.10, or 0.15 μg/mL), NAM (5 mM), and guanine (0.5 mM) were added optionally.

AUTHOR CONTRIBUTIONS

Conceptualization: T.A. and M.O. *Methodology*: T.A. and M.O. Validation: T.A., T.Y., and M.O. *Formal analysis*: T.A. and T.Y. *Investigation*: T.A., T.Y., and M.O. *Data curation*: T.A. and T.Y. *Writing—original draft preparation*: T.A. and M.O. *Writing—review and editing*: T.A. and M.O. *Visualization*: T.A. *Supervision*: M.O. *Project administration*: M.O. *Funding acquisition*: T.A. and M.O. All authors have read and agreed to the published version of the manuscript.

ACKNOWLEDGMENTS

We thank Dr. Karaya for supervising the microarray experiment. This study was supported by JSPS KAKENHI Grant Number JP22H02301 and JP21J15569, and by Institute for Fermentation, Osaka (IFO) Grant Number G-2022-2-18.

CONFLICT OF INTEREST STATEMENT

The authors declare no conflict of interest.

ORCID

Masaya Oki https://orcid.org/0000-0002-5563-0443

REFERENCES

Amano, T., Hirata, T., Falco, G., Monti, M., Sharova, L. V., Amano, M., Sheer, S., Hoang, H. G., Piao, Y., Stagg, C. A., Yamamizu, K., Akiyama, T., & Ko, M. S. (2013). Zscan4 restores the developmental potency of embryonic stem cells. *Nature Communications*, *4*, 1966. https://doi.org/10.1038/ncomms2966

Avalos, J. L., Bever, K. M., & Wolberger, C. (2005). Mechanism of sirtuin inhibition by nicotinamide: Altering the NAD(+) cosubstrate specificity of a Sir2 enzyme. *Molecular Cell*, *17*(6), 855–868. https://doi.org/10.1016/j.molcel.2005.02.022

Beltran, T., Shahrezaei, V., Katju, V., & Sarkies, P. (2020). Epimutations driven by small RNAs arise frequently but most have limited duration in *Caenorhabditis elegans*. *Nature Ecology & Evolution*, *4*(11), 1539–1548. https://doi.org/10.1038/s41559-020-01293-z

Bheda, P., Aguilar-Gomez, D., Becker, N. B., Becker, J., Stavrou, E., Kukhtevich, I., Höfer, T., Maerkl, S., Charvin, G., Marr, C., Kirmizis, A., & Schneider, R. (2020). Single-cell tracing dissects regulation of maintenance and inheritance of transcriptional reinduction memory. *Molecular Cell*, *78*(5), 915–925 e917. https://doi.org/10.1016/j.molcel.2020.04.016

Bitterman, K. J., Anderson, R. M., Cohen, H. Y., Latorre-Esteves, M., & Sinclair, D. A. (2002). Inhibition of silencing and accelerated aging by nicotinamide, a putative negative regulator of yeast sir2 and human SIRT1. *Journal of Biological Chemistry*, *277*(47), 45099–45107. https://doi.org/10.1074/jbc.M205670200

Boeke, J. D., LaCroute, F., & Fink, G. R. (1984). A positive selection for mutants lacking orotidine-5′-phosphate decarboxylase activity in yeast: 5-fluoro-orotic acid resistance. *Molecular and General Genetics*, *197*(2), 345–346. https://doi.org/10.1007/BF00330984

Bolstad, B. M., Irizarry, R. A., Astrand, M., & Speed, T. P. (2003). A comparison of normalization methods for high density oligonucleotide array data based on variance and bias. *Bioinformatics*, *19*(2), 185–193. https://doi.org/10.1093/bioinformatics/19.2.185

Connell, Z., Parnell, T. J., McCullough, L. L., Hill, C. P., & Formosa, T. (2022). The interaction between the Spt6-tSH2 domain and Rpb1 affects multiple functions of RNA polymerase II. *Nucleic Acids Research*, *50*(2), 784–802. https://doi.org/10.1093/nar/gkab1262

Davis, C. A., & Ares, M., Jr. (2006). Accumulation of unstable promoter-associated transcripts upon loss of the nuclear exosome subunit Rrp6p in *Saccharomyces cerevisiae*. *Proceedings of the National Academy of Sciences of the United States of America*, *103*(9), 3262–3267. https://doi.org/10.1073/pnas.0507783103

Donze, D., Adams, C. R., Rine, J., & Kamakaka, R. T. (1999). The boundaries of the silenced HMR domain in *Saccharomyces cerevisiae*. *Genes & Development*, *13*(6), 698–708. https://doi.org/10.1101/gad.13.6.698

Donze, D., & Kamakaka, R. T. (2001). RNA polymerase III and RNA polymerase II promoter complexes are heterochromatin barriers in *Saccharomyces cerevisiae*. *EMBO Journal*, *20*(3), 520–531. https://doi.org/10.1093/emboj/20.3.520

Ellahi, A., Thurtle, D. M., & Rine, J. (2015). The chromatin and transcriptional landscape of native *Saccharomyces cerevisiae* telomeres and subtelomeric domains. *Genetics*, *200*(2), 505–521. https://doi.org/10.1534/genetics.115.175711

Escobar-Henriques, M., & Daignan-Fornier, B. (2001). Transcriptional regulation of the yeast gmp synthesis pathway by its end products. *Journal of Biological Chemistry*, *276*(2), 1523–1530. https://doi.org/10.1074/jbc.M007926200

Escobar-Henriques, M., Daignan-Fornier, B., & Collart, M. A. (2003). The critical cis-acting element required for IMD2 feedback regulation by GDP is a TATA box located 202 nucleotides upstream of the transcription start site. *Molecular and Cellular Biology*, *23*(17), 6267–6278. https://doi.org/10.1128/MCB.23.17.6267-6278.2003

Gartenberg, M. R., & Smith, J. S. (2016). The nuts and bolts of transcriptionally silent chromatin in *Saccharomyces cerevisiae*. *Genetics*, *203*(4), 1563–1599. https://doi.org/10.1534/genetics.112.145243

Ghidelli, S., Donze, D., Dhillon, N., & Kamakaka, R. T. (2001). Sir2p exists in two nucleosome-binding complexes with distinct deacetylase activities. *EMBO Journal*, *20*(16), 4522–4535. https://doi.org/10.1093/emboj/20.16.4522

Hedstrom, L. (1999). IMP dehydrogenase: Mechanism of action and inhibition. *Current Medicinal Chemistry*, *6*(7), 545–560. https://www.ncbi.nlm.nih.gov/pubmed/10390600

Hyle, J. W., Shaw, R. J., & Reines, D. (2003). Functional distinctions between IMP dehydrogenase genes in providing mycophenolate resistance and guanine prototrophy to yeast. *Journal of Biological Chemistry*, *278*(31), 28470–28478. https://doi.org/10.1074/jbc.M303736200

Imai, S., Armstrong, C. M., Kaeberlein, M., & Guarente, L. (2000). Transcriptional silencing and longevity protein Sir2 is an NAD-dependent histone deacetylase. *Nature*, *403*(6771), 795–800. https://doi.org/10.1038/35001622

Irizarry, R. A., Bolstad, B. M., Collin, F., Cope, L. M., Hobbs, B., & Speed, T. P. (2003). Summaries of Affymetrix GeneChip probe level data. *Nucleic Acids Research*, *31*(4), e15. https://doi.org/10.1093/nar/gng015

Irizarry, R. A., Hobbs, B., Collin, F., Beazer-Barclay, Y. D., Antonellis, K. J., Scherf, U., & Speed, T. P. (2003). Exploration, normalization, and summaries of high density oligonucleotide array probe level data. *Biostatistics*, *4*(2), 249–264. https://doi.org/10.1093/biostatistics/4.2.249

Jenks, M. H., O'Rourke, T. W., & Reines, D. (2008). Properties of an intergenic terminator and start site switch that regulate IMD2 transcription in yeast. *Molecular and Cellular Biology*, *28*(12), 3883–3893. https://doi.org/10.1128/MCB.00380-08

Jenks, M. H., & Reines, D. (2005). Dissection of the molecular basis of mycophenolate resistance in *Saccharomyces cerevisiae*. *Yeast*, *22*(15), 1181–1190. https://doi.org/10.1002/yea.1300

Kamata, K., Ayano, T., & Oki, M. (2023). Spt3 and Spt8 are involved in the formation of a silencing boundary by interacting with TATA-binding protein. *Biomolecules*, *13*(4), 619. https://doi.org/10.3390/biom13040619

Kamata, K., Shinmyozu, K., Nakayama, J. I., Hatashita, M., Uchida, H., & Oki, M. (2016). Four domains of Ada1 form a heterochromatin boundary through different mechanisms. *Genes to Cells*, *21*(10), 1125–1136. https://doi.org/10.1111/gtc.12421

Kanada, F., Ogino, Y., Yoshida, T., & Oki, M. (2020). A novel tracking and analysis system for time-lapse cell imaging of *Saccharomyces cerevisiae*. *Genes & Genetic Systems*, *95*(2), 75–83. https://doi.org/10.1266/ggs.19-00061

Kimura, A., & Horikoshi, M. (2004). Partition of distinct chromosomal regions: Negotiable border and fixed border. *Genes to Cells*, *9*(6), 499–508. https://doi.org/10.1111/j.1356-9597.2004.00740.x

Kimura, A., Umehara, T., & Horikoshi, M. (2002). Chromosomal gradient of histone acetylation established by Sas2p and Sir2p functions as a shield against gene silencing. *Nature Genetics*, *32*(3), 370–377. https://doi.org/10.1038/ng993

Ko, M. S. (2016). Zygotic genome activation revisited: Looking through the expression and function of Zscan4. *Current Topics in Developmental Biology*, *120*, 103–124. https://doi.org/10.1016/bs.ctdb.2016.04.004

Kopcewicz, K. A., O'Rourke, T. W., & Reines, D. (2007). Metabolic regulation of IMD2 transcription and an unusual DNA element that generates short transcripts. *Molecular and Cellular Biology*, *27*(8), 2821–2829. https://doi.org/10.1128/MCB.02159-06

Kuehner, J. N., & Brow, D. A. (2008). Regulation of a eukaryotic gene by GTP-dependent start site selection and transcription attenuation. *Molecular Cell*, *31*(2), 201–211. https://doi.org/10.1016/j.molcel.2008.05.018

Longtine, M. S., Fares, H., & Pringle, J. R. (1998). Role of the yeast Gin4p protein kinase in septin assembly and the relationship between septin assembly and septin function. *Journal of Cell Biology*, *143*(3), 719–736. https://doi.org/10.1083/jcb.143.3.719

Mano, Y., Kobayashi, T. J., Nakayama, J., Uchida, H., & Oki, M. (2013). Single cell visualization of yeast gene expression shows correlation of epigenetic switching between multiple heterochromatic regions through multiple generations. *PLoS Biology*, *11*(7), e1001601. https://doi.org/10.1371/journal.pbio.1001601

McPhillips, C. C., Hyle, J. W., & Reines, D. (2004). Detection of the mycophenolate-inhibited form of IMP dehydrogenase in vivo. *Proceedings of the National Academy of Sciences of the United States of America*, *101*(33), 12171–12176. https://doi.org/10.1073/pnas.0403341101

Mitsumori, R., Ohashi, T., Kugou, K., Ichino, A., Taniguchi, K., Ohta, K., Uchida, H., & Oki, M. (2016). Analysis of novel Sir3 binding regions in *Saccharomyces cerevisiae*. *Journal of Biochemistry*, *160*(1), 11–17. https://doi.org/10.1093/jb/mvw021

Oki, M., & Kamakaka, R. T. (2002). Blockers and barriers to transcription: Competing activities? *Current Opinion in Cell Biology*, *14*(3), 299–304. https://doi.org/10.1016/s0955-0674(02)00327-7

Oki, M., & Kamakaka, R. T. (2005). Barrier function at HMR. *Molecular Cell*, *19*(5), 707–716. https://doi.org/10.1016/j.molcel.2005.07.022

Oki, M., Valenzuela, L., Chiba, T., Ito, T., & Kamakaka, R. T. (2004). Barrier proteins remodel and modify chromatin to restrict silenced domains. *Molecular and Cellular Biology*, *24*(5), 1956–1967. https://doi.org/10.1128/MCB.24.5.1956-1967.2004

Rothstein, R. (1991). Targeting, disruption, replacement, and allele rescue: Integrative DNA transformation in yeast. *Methods in Enzymology*, *194*, 281–301. https://doi.org/10.1016/0076-6879(91)94022-5

Rusche, L. N., Kirchmaier, A. L., & Rine, J. (2003). The establishment, inheritance, and function of silenced chromatin in *Saccharomyces cerevisiae*. *Annual Review of Biochemistry*, *72*, 481–516. https://doi.org/10.1146/annurev.biochem.72.121801.161547

Saxton, D. S., & Rine, J. (2022). Distinct silencer states generate epigenetic states of heterochromatin. *Molecular Cell*, *82*(19), 3566–3579 e3565. https://doi.org/10.1016/j.molcel.2022.08.002

Shaw, R. J., & Reines, D. (2000). Saccharomyces cerevisiae transcription elongation mutants are defective in PUR5 induction in response to nucleotide depletion. *Molecular and Cellular Biology*, *20*(20), 7427–7437. https://doi.org/10.1128/MCB.20.20.7427-7437.2000

Shaw, R. J., Wilson, J. L., Smith, K. T., & Reines, D. (2001). Regulation of an IMP dehydrogenase gene and its overexpression in drug-sensitive transcription elongation mutants of yeast. *Journal of Biological Chemistry*, *276*(35), 32905–32916. https://doi.org/10.1074/jbc.M105075200

Smith, J. S., & Boeke, J. D. (1997). An unusual form of transcriptional silencing in yeast ribosomal DNA. *Genes & Development*, *11*(2), 241–254. https://doi.org/10.1101/gad.11.2.241

Steinmetz, E. J., Warren, C. L., Kuehner, J. N., Panbehi, B., Ansari, A. Z., & Brow, D. A. (2006). Genome-wide distribution of yeast RNA polymerase II and its control by Sen1 helicase. *Molecular Cell*, *24*(5), 735–746. https://doi.org/10.1016/j.molcel.2006.10.023

Suka, N., Luo, K., & Grunstein, M. (2002). Sir2p and Sas2p opposingly regulate acetylation of yeast histone H4 lysine16 and spreading of heterochromatin. *Nature Genetics*, *32*(3), 378–383. https://doi.org/10.1038/ng1017

Sun, J. Q., Hatanaka, A., & Oki, M. (2011). Boundaries of transcriptionally silent chromatin in *Saccharomyces cerevisiae*. *Genes & Genetic Systems*, *86*(2), 73–81. https://doi.org/10.1266/ggs.86.73

Torres-Garcia, S., Yaseen, I., Shukla, M., Audergon, P., White, S. A., Pidoux, A. L., & Allshire, R. C. (2020). Epigenetic gene silencing by heterochromatin primes fungal resistance. *Nature*, *585*(7825), 453–458. https://doi.org/10.1038/s41586-020-2706-x

Wilson, R., Le Bourgeois, M., Perez, M., & Sarkies, P. (2023). Fluctuations in chromatin state at regulatory loci occur spontaneously under relaxed selection and are associated with epigenetically inherited variation in *C. elegans* gene expression. *PLoS Genetics*, *19*(3), e1010647. https://doi.org/10.1371/journal.pgen.1010647

Woods, R. A., Roberts, D. G., Friedman, T., Jolly, D., & Filpula, D. (1983). Hypoxanthine: Guanine phosphoribosyltransferase

mutants in *Saccharomyces cerevisiae*. *Molecular and General Genetics*, *191*(3), 407–412. https://doi.org/10.1007/BF00425755

Yaseen, I., White, S. A., Torres-Garcia, S., Spanos, C., Lafos, M., Gaberdiel, E., Yeboah, R., El Karoui, M., Rappsilber, J., Pidoux, A. L., & Allshire, R. C. (2022). Proteasome-dependent truncation of the negative heterochromatin regulator Epe1 mediates antifungal resistance. *Nature Structural & Molecular Biology*, *29*(8), 745–758. https://doi.org/10.1038/s41594-022-00801-y

Zalzman, M., Falco, G., Sharova, L. V., Nishiyama, A., Thomas, M., Lee, S. L., Stagg, C. A., Hoang, H. G., Yang, H.-T., Indig, F. E., Wersto, R. P., & Ko, M. S. (2010). Zscan4 regulates telomere elongation and genomic stability in ES cells. *Nature*, *464*(7290), 858–863. https://doi.org/10.1038/nature08882

SUPPORTING INFORMATION

Additional supporting information can be found online in the Supporting Information section at the end of this article.

How to cite this article: Ayano, T., Yokosawa, T., & Oki, M. (2024). GTP-dependent regulation of heterochromatin fluctuations at subtelomeric regions in *Saccharomyces cerevisiae*. *Genes to Cells*, *29*(3), 217–230. https://doi.org/10.1111/gtc.13094